Supplemental Text

Analysis of the ice core samples

The six ice cores were transported frozen to the cold rooms at The Ohio State University (OSU) where the entire lengths of five cores were cut into a continuous sequence of samples (NIF2, 2197 samples; NIF3, 1980 samples; SIF1, 706 samples; SIF2, 834 samples; FWG, 343 samples). Complete sets of samples were analyzed for oxygen and hydrogen isotopic ratios ($\delta^{18}O$, δD), and concentrations of insoluble microparticles (dust), anions (fluoride, chloride, nitrate and sulfate, or F^-, Cl^-, NO_3^- and SO_4^{2-}, respectively) and cations (sodium, ammonium, potassium, magnesium and calcium, or Na^+, NH_4^+, K^+, Mg^{2+} and Ca^{2+}, respectively). SIF1 was not analyzed for dust and the sixth core, NIF1 (drilled one meter from NIF2) has been reserved for other measurements such as AMS ^{14}C and pollen.

Dating the Kilimanjaro Cores

As noted in the main text dating the Kilimanjaro required significant effort. Here we have included additional material to complement the dating discussion in the paper. These comments follow the dating discussion in chronological order.

The net down wasting of the NIF (as discussed in the main text) over the past four decades can only be reconciled with the presence of the ^{36}Cl chronostratigraphic layer by a massive, temporary deposition of low density snow. It is nearly certain that this snow fell in association with the heavy rainfall in October and November 1961 that caused Lake Victoria to rise 2.5 m (1961 to 1964), Lake Albert to rise 3.5 m (1961-1963) and Lake Tanganyika to rise 2.5 m (1961 to 1964) *(1s)*.

Application of the Nye model

Establishing time scales for the five Kilimanjaro cores required constructing a time scale for NIF3 and then referencing the other four cores to this 'master chronology' by the depth-to-depth transfers using common $\delta^{18}O$ features discussed in the text and shown in Figure 2. We used the simplest age-modeling for a steady-state glacier of constant accumulation, the formula first introduced by Nye *(8, 9)*, relating the age, t, at any given depth, z, as

$$t = \{h \cdot \ln[h/(h-z)]/a\}, \qquad \text{(Eq. 1)}$$

where 'a' is the long-term surface accumulation rate and 'h' is the ice cap thickness (in m ice eq.). For application of the Nye model the time-averaged ice thickness in the vicinity of the more centrally located NIF3 site (Fig. 1), is assumed to be ~50 m, roughly its current thickness, although the ice thickness has undoubtedly fluctuated in the past. The exponential age-depth relation in Eq. 1 approaches infinity near bedrock, thus requiring construction of a finite approximation for the lower part of the core (discussed below).

Assigning time horizons

Three time horizons were chosen to guide both this approximation and application of the model. The year 1950 A.D., also representing the origin of the calibrated-radiocarbon timescale, was assigned to the depth of 1.6 m (NIF2), consistent with the ^{36}Cl bomb horizon (Fig. S2b). This translates to 1.13 m in NIF3 by $\delta^{18}O$ matching. Because of the large fluctuations in surface accumulation/ablation apparent at all sites since 1950, it was inappropriate to apply an age model from the surface since the surface age is likely to be different at each site. Therefore, 1.13 m was subtracted from all depths in NIF3 prior to application of the age-depth model. Note that the model-derived depth of the 1325 A.D. horizon (discussed in printed text) yields an average annual accumulation, a, of 0.01275 m of ice equivalent for the 1950 to 1325 A.D. interval.

Further support for assigning the 1325 A.D. horizons comes from comparing the upper part of the Kilimanjaro $\delta^{18}O$ record with the history of fluctuations in other regional and hemispheric proxies that suggest that the late Neoglacial cooling (i.e., Little Ice Age, LIA) was characterized by two extreme phases. The faunal record of SST from a core off the coast of West Africa suggests two cool periods centered at ~1600 and ~1250 A.D. *(2s)*. There is additional evidence for the early LIA cool phase between 1100 and 1350 A.D. in proxy records from widely separated locales such as Baffin Bay, European Alps, South American Andes, and New Zealand *(3s)*.

Assuming that the earliest isotopic minimum is correlative with the Wolf Minimum leads to the logical conclusion that the more recent period of depleted $\delta^{18}O$ values centered at 3.55 m in NIF3 (4.35 m NIF2) likely corresponds to the Maunder Minimum. Therefore, the intermediate $\delta^{18}O$-depletion signature in NIF3 at 5.6-6.0 m (less evident in NIF2 at 6.9-7.3 m) may reflect the Spörer Minimum (1450-1530 A.D.). The combination of higher lake levels *(10)* and a pollen-inferred LIA cooling of ~2°C reported from southeastern Ethiopia *(4s)*, along depleted $\delta^{18}O$ from the Kilimanjaro cores, suggests that the LIA was cool and wet in tropical East Africa.

As discussed in the main text the basal age of 11.7 ka was assigned by comparison of the NIF3 isotope profile and that in the well-dated Soreq record. The Soreq cave record reflects regional wetness (less negative $\delta^{18}O$ recording dry conditions) and a credible inverse correlation between the Soreq Cave record and NIF3 $\delta^{18}O$ (Fig. 4c,d) was produced following the finite-Nye model application. Confidence that the NIF3 time scale is broadly correct derives from the common sequence of events between 8.3 and 4.0 ka that occur nearly concurrently with other independently-dated records. Also, the predominant Holocene climate history (deteriorating from a Climatic Optimum to the

Neoglacial Age) is evident and similar to that from the independently dated Huascarán ice core (Fig. 4b) at a comparable latitude in Peru.

Finite approximation of the age of the bottom ~6 meters of NIF 3

With the basal age constrained to 11.7 ka in NIF3, the Nye model age formula was applied only down to the point where continued layer thinning was necessarily terminated and a constant layer thickness was assigned. The age of this finite termination point of the exponential model is determined by rearranging Eq. 1 to define the intermediate target depth,

$$z_f = h - h \cdot e[\exp(-t_f \cdot a/h)], \qquad \text{(Eq. 2)}$$

where t_f represents the age (in ka before 1950) of the Nye model termination. The thickness of the portion of basal ice to be age-dated by constant accumulation is represented alternately by either side of the following equality:

$$(dz_f/dt) \cdot (11.7 - t_f) = (h - z_f) \qquad \text{(Eq. 3)}$$

where (dz_f/dt) represents the 'instantaneous' layer thickness at the termination point. From Eq. 2, (dz_f/dt) is also equivalent to $a \cdot e[\exp(-t_f \cdot a/h)]$ and by substitution, Eq. 3 reduces to

$$t_f = 11.7 - h/a.$$

Given that h = 48.97-1.13 (47.84) and a = .01275 m/yr, t_f = 7.95 ka (~8.0 ka). This age represents a depth of 43.4 m NIF3, such that the finite approximation is only applied to the basal 5.6 m of the NIF3 site, and not at all to the other four cores.

Discussion of the anomalous ice in SIF2 (mentioned in the caption for Figure 3)

The gap in the SIF2 record represents a 1-m section of the core (16.5-17.5 m depth) lost during field operations. The 'asterisk' on the SIF2 record (Fig. 3) at ~1600 A.D. indicates the stratigraphic position of a ~6 m section of 'rogue ice' that was removed from the record because the isotopic signature was unique within the set of five cores. A large

dust layer (similar to, but less concentrated than the NIF3 event at 32.5 m) was found at the same stratigraphic level in SIF1 suggesting that the anomalous isotopic signature and the high dust event were related. Continuous cross-correlation between SIF1 and NIF3 did not suggest an accumulation hiatus of long duration. Therefore, we concluded that the 6m interval in SIF2 likely represents a brief mass wasting or crevasse formation event that was subsequently and rapidly filled in once continuous accumulation resumed. This feature would likely have appeared similar to the one visible in the 2000 aerial photograph (not shown, but evident in the 2000 ice extent for NIF shown in Figure 1). The bottom age of the Fηrtwangler Glacier (FWG) is within 100 years of this disturbance event. The absence of FWG suggests that all ice from the interior of the Kibo crater was removed at this time which, from cosmogenic proxies, is known to be a brief period of high solar output (see topmost curve in Figure 3). We have mentioned this anomalous feature for completeness and to highlight that the matching of isotopic features among these five cores is quite credible and allows easy identification of stratigraphic discontinuities due to disruption at one site and not others.

Discussion of the termination of the ~4.2 ka arid period

The termination of the 300 year dry period and reestablishment of wetter conditions in East Africa ca. 1970 B.C. is evidenced by rising lake levels and also from written records in Egypt. Lake Turkana (Rudolf) levels rose at least 75 m and overflowed into the Nile system, while the White Nile was 2-3 m higher than at present, with a discharge 50 times greater than now *(5s)*. In the cataracts of Sudanese Nubia there are at least twenty-seven inscriptions dating between 1840 and 1770 B. C. that note floods 8-11 m higher than those of the present (*6s)*.

References cited in the Supplementary Material

1s. G. W. Kite, *Hydrological Sciences Bulletin* **26**, 233 (1981).

2s. P. deMenocal, J. Ortiz, T. Guilderson, M. Sarnthein, *Science* **288**, 2198 (2000).

3s. J. M. Grove, *The Little Ice Age*, (Methuen, London, 1988), pp. 349-353.

4s. R. Bonnefille, U. Mohammed, *Palaeogeography, Palaeoclimatology, Palaeoecology* **109**, 31 (1994).

5s. K. W. Butzer, in *Third Millennium BC Climate Change and Old World Collapse,* H. N. Dalfes, G. Kukla, H. Wiess, Eds. (NATO ASI Series I: Global Environmental Change, Vol 49, Springer, Berlin, 199x), pp. 245-296.

6s. B. Bell, *Am. J. Archaeology* **79**, 223 (1971).

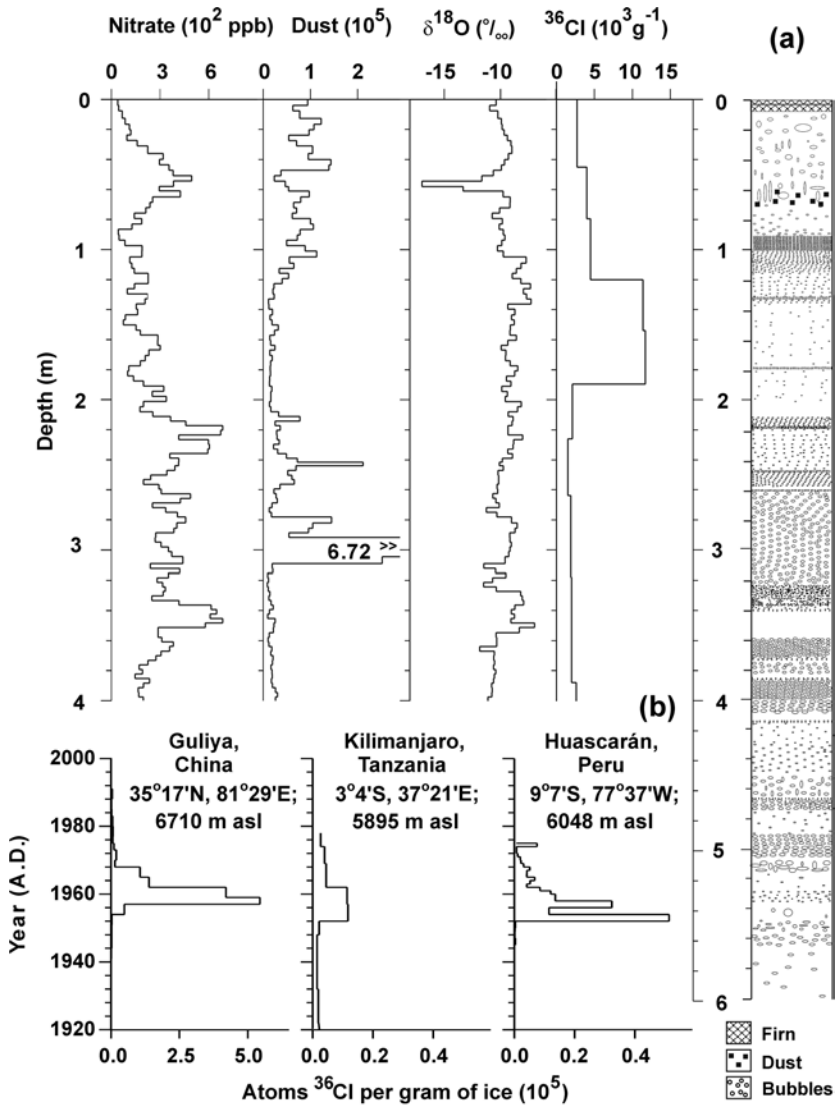

Figure S1. The individual sample values for nitrate, dust, $\delta^{18}O$, and ^{36}Cl are shown for the upper 4 meters of the NIF2 core along with the visible stratigraphy in the upper 6 meters of NIF3. Figure 2(b) shows the ^{36}Cl peak associated with the Ivy test in the NIF2 core along with the ^{36}Cl peaks in the ice cores from Huascarán, Peru (–9°S) and Guliya ice cap, China (–35°N). The latter two cores were dated very accurately using seasonally varying constituents.

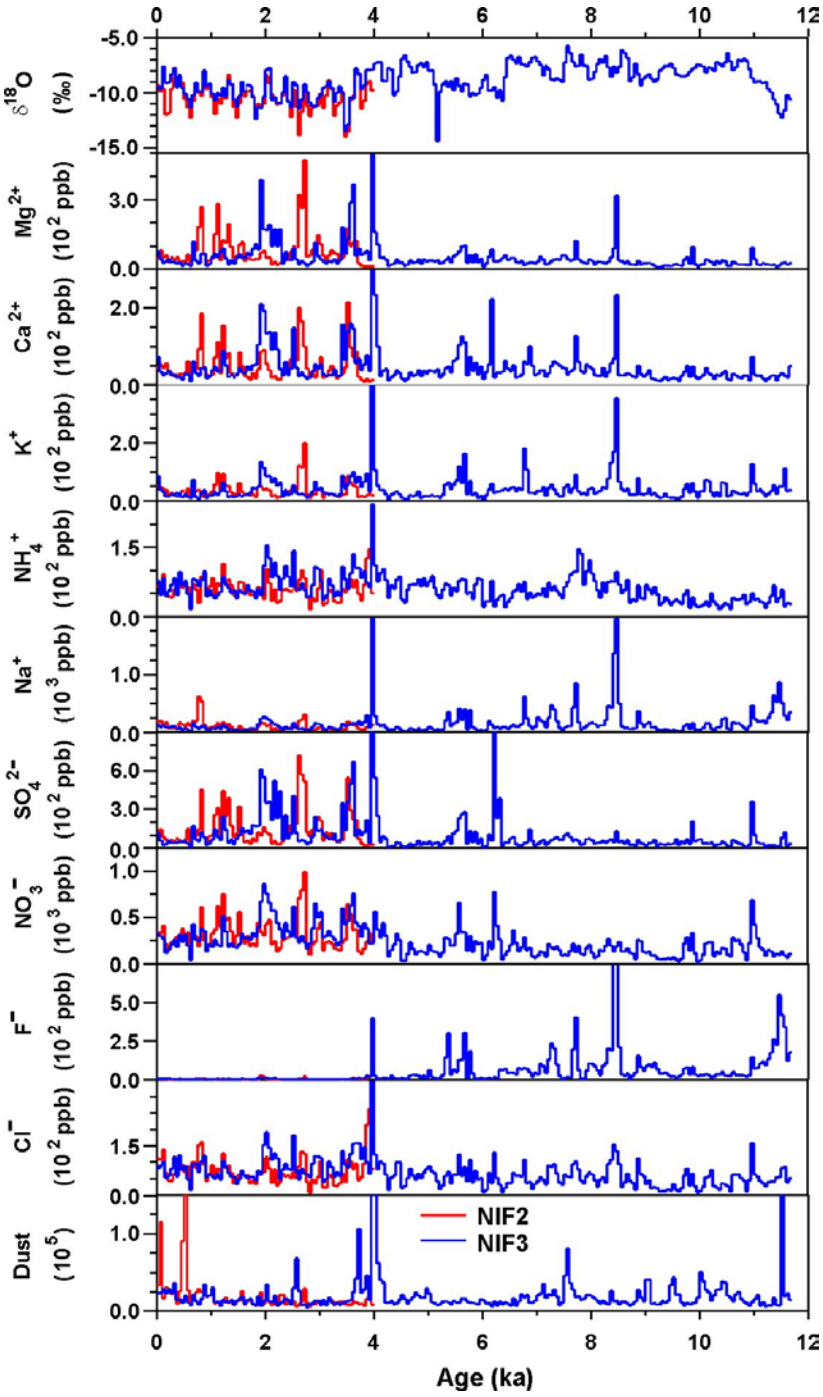

Figure S2. The 50-year averages of $\delta^{18}O$, Mg^{2+}, Ca^{2+}, K^{+}, NH_4^{+}, Na^{+}, SO_4^{2-}, NO_3^{-}, F^{-}, Cl^{-} and dust (diameters from 0.63 to 16.0 μm per ml sample) are shown for the entire NIF2 record (red) and the entire NIF3 record (blue).

Table S1. These are all the ^{14}C dates measured on the Kilimanjaro cores. Note the small sizes of the samples. **A**nalyses were made at Lawrence Livermore National Laboratory unless noted by $^{+}$ for Woods Hole Oceanographic Institution. $^{14}C_{cal}$ ages were calculated using Method A *(11)*. The ^{14}C dates from the bottom of NIF3 were used merely to support the lack of glacial stage ice inferred from the absence of depleted $\delta^{18}O$ and the likelihood of an early Holocene age for ice near the bottom. We also used the dates near the bottom of NIF1 to support the age of –4 ka inferred from the $\delta^{18}O$ match to NIF3 (Fig. 2b,c). The * implies modern (1950 or more recent).

Core	Depth (m)	Carbon (mg)	^{14}C ages (yr. BP) $\pm 1\sigma$	$^{14}C_{cal}$ (rounded) ages with [1σ range]
NIFC1	23.95-25.05	0.06	4410±140	5020 [5298, 4837]
NIFC1	31.79-32.76	0.09	1700±320	1580 [1988, 1292]
NIFC1^{+}	35.33-36.33	0.02	820±170	730 [927, 571]
NIFC1	40.42-41.67	0.08	3630±130	3950 [4146, 3728]
NIFC1	46.27-46.86	0.05	1830±130	1760 [1919, 1571
NIFC1	50.01-51.03	0.05	5280±170	6090 [6281, 5906]
NIFC1^{+}	50.01-51.03	0.03	3710±180	4050 [4351, 3781]
NIFC3	19.57-20.5	0.05	4150±470	4700 [5318, 3986]
NIFC3	32.52	0.27	160±40	“modern” [282, 1]
NIFC3	32.52 (replicate)	0.10	170±70	“modern” [294, 0*]
NIFC3	32.87-33.97	0.11	2400±70	2360 [2707, 2347]

NIFC3	46.9-47.9	0.17	8100±180	9010 [9397, 8657]
NIFC3	47.9-48.97	0.05	5870±130	6700 [6852, 6500]
NIFC3	47.9-48.97 (repl)	0.05	3730±110	4090 [4241, 3911]
NIFC3	47.9-48.97	0.03	8280±380	9360 [9596, 8646]
SIFC1	9.7	0.114	190±50	“modern” [297, 0*]
$SIFC1^{+}$	9.7	0.22	880±60	780 [910 (787, 729]

Table S2. Concentrations of dust, $\delta^{18}O$ and chemical species for the ~4.0 ka dust event and their comparison with the whole core average concentrations.

Physical or Chemical Parameter	Dust Event Average	Total Core Average (without dust event)	Ratio of Dust Event to Total Core Average
Dust > 0.63μm	2196 $x10^5$	0.350 $x10^5$	6272
$\delta^{18}O$	-10.64‰	-9.27‰	-1.4‰ (difference)
F^- (ppb)	3624	32	112
Cl^- (ppb)	7245	73	100
NO_3^- (ppb)	252	275	1
SO_4^{2-} (ppb)	27,117	117	231
Na^+ (ppb)	33,679	116	291
NH_4^+ (ppb)	1832	65	28
K^+ (ppb)	9944	39	255
Mg^{2+} (ppb)	840	6	143
Ca^{2+} (ppb)	6159	48	183